NJC

PAPER

View Article Online
View Journal | View Issue

Cite this: *New J. Chem.*, 2014, **38**, 1655

Stereoselective synthesis of *Z*-acrylonitrile derivatives: catalytic and acetylcholinesterase inhibition studies†

Mehtab Parveen,*[a] Ali Mohammed Malla,[a] Mahboob Alam,[a] Musheer Ahmad[b] and Shahnawaz Rafiq[b]

Received (in Montpellier, France) 8th November 2013,
Accepted 13th January 2014

DOI: 10.1039/c3nj01384g

www.rsc.org/njc

In the present study, a focused library of (*Z*)-acrylonitrile analogues (library A & B) were synthesized, which were typically accessed *via* a facile Knoevenagel condensation between *p*-nitrophenylacetonitrile and appropriately substituted aromatic aldehydes (**1a–i**) and 3-formyl chromones (**3a–c**). This new synthetic eco-friendly approach resulted in a remarkable improvement in the synthetic efficiency (83–92% yield), high purity, minimizing the production of chemical wastes without using highly toxic reagents for the synthesis and, more notably, it improved the selectivity for (*Z*)-acrylonitrile derivatives. By performing DFT calculations, it was found that the (*Z*)-isomer of compound **2b** is stabilized by 2.61 kcal mol^{-1} more than the (*E*)-isomer. All of the compounds were tested for acetylcholinesterase (AChE) inhibition. Compounds **2a** and **4c**, displayed the strongest inhibition, with IC_{50} values of 0.20 μM and 0.22 μM respectively. The methoxy group at the *para*-position of phenyl ring A was found to be essential for AChE inhibition.

1. Introduction

Carbon–carbon bond formation reactions are the most important reactions in organic synthesis.[1–3] The Knoevenagel condensation between aldehydes or ketones with activated methylene compounds is one of the reactions which facilitates C–C bond formation[4,5] and has been exploited in the synthesis of some vital drugs such as entacapone,[6] pioglitazone[7] and lumefantrine[8] (Fig. 1). Over the past few decades there has been an increasing prevalence in the number of biologically active compounds that contain an acrylonitrile moiety.[9,10] The reactivity of heteroarylacetonitriles has been exploited for the synthesis of some nitrogen-bridged heterocycles.[11] Acetonitrile derivatives are useful intermediates and scaffolds which possess a wide range of promising biological properties such as antiproliferative,[12] antifungal,[13] antitumor,[14] antibacterial,[15] antitubercular,[16] antioxidative,[17] insecticidal,[18] spasmolytic,[19] estrogenic,[20] hypotensive,[21] tuberculostatic,[22] antitrichomonal[23] and antiparasitic[24] properties.

It was recently reported that 2-acetyl-3-(6-methoxybenzothiazo)-2-yl-amino-acrylonitrile (AMBAN) possesses significant anti-proliferative activity and is a potent inducer of programmed cell death in human leukemia cells.[25] Acrylonitrile derivatives have been recently documented as selective acetylcholinesterase inhibitors.[26] The immense biological importance inspired researchers, therefore, to synthesize them and study their potential biological activities.

The synthesis of acrylonitrile compounds has previously been achieved by the use of Wittig reactions,[27] McMurry coupling reactions[28] and the Heck reaction.[29] The recognition of diethyl amine as a catalyst, first by Knoevenagel,[1] paved the way for the development of a large number of catalysts[30–33] and reaction conditions.[34–36] Despite the various methods, the Knoevenagel condensation is a simple and straightforward approach for the synthesis of acrylonitrile derivatives.[37,38] This method involves the acid or base-catalyzed condensation of active methylene moieties with carbonyl compounds. In the quest to achieve higher efficiency, several catalysts and reaction conditions were tried, including the use of microwaves,[39] Brønsted acid catalysts,[40] Lewis acids such as $MgBr_2{\cdot}OEt_2$,[41] $SnCl_2$,[42] silica-supported catalysts,[43,44] bases such as NaOEt,[45] piperidine[46] and potassium sorbate.[47] Earlier investigations required long reaction times, the use of hazardous reagents and tedious workup procedures. In view of the numerous biological applications of acrylonitrile derivatives, the development of a simple and convenient protocol is of considerable interest.

In recent years, the use of reagents and catalysts supported on solid supports[48–50] has received considerable attention due to growing environmental concerns. Such reagents not only

[a] *Department of Chemistry, Aligarh Muslim University, Aligarh, 202002, India. E-mail: mehtab.organic2009@gmail.com; Tel: +91 09897179498*
[b] *Indian Institute of Technology (IIT), Kanpur, 208016, India*

† Electronic supplementary information (ESI) available. CCDC 963259. For ESI and crystallographic data in CIF or other electronic format see DOI: 10.1039/c3nj01384g

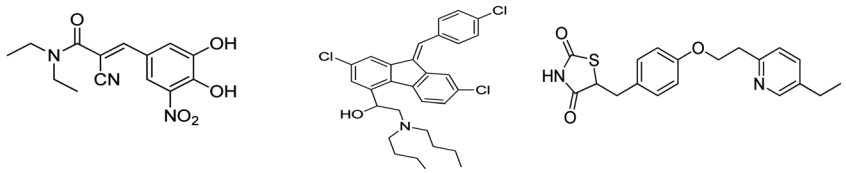

Fig. 1 Knoevenagel assisted synthesis of some vital drugs.

simplify the purification processes but also help in preventing the discharge of toxic reaction residues into the environment. In this respect, silica chloride (SiO_2–Cl) is an attractive candidate. It is a well known catalyst in organic synthesis and has been documented in several organic transformations.[51–53] Silica chloride was prepared by employing standard procedures depicted in the literature.[54] To a well stirred oven-dried silica gel in dry dichloromethane, thionyl chloride was added dropwise at room temperature, and the evolution of profuse amounts of HCl and SO_2 occurred instantaneously. After stirring for 2 hours, the solvent was removed to dryness under reduced pressure. The silica chloride thus synthesized was used in the following experiments. The mechanistic pathway for the preparation of silica chloride is shown in Scheme 1.[55] It possesses environmentally benign properties such as non-toxicity, biocompatibility, recyclability, physiological inertness, inexpensiveness and thermal stability. This new synthetic strategy resulted in a remarkable improvement in the synthetic efficiency and more notably, it enhanced the selectivity for (*Z*)-acrylonitrile derivatives, and minimized the production of chemical waste without using highly toxic reagents for the synthesis. In addition to efficacy, a major requirement of novel supported reagents concerns their reusability, a factor that has significant environmental and economic impact since the most costly components in a chemical reaction are often not the starting materials but the catalyst.[56,57] The Si–Cl bond is labile and can give rise to Lewis acid centers on silica. The Cl is displaced selectively by the carbonyl oxygen of the aldehyde by a nucleophilic substitution reaction, generating a cationic centre on the carbonyl carbon, which is believed to be easily attacked by the nucleophile, *i.e.* the imide form of *p*-nitrophenylacetonitrile,[58] to give the corresponding acrylonitrile derivatives.

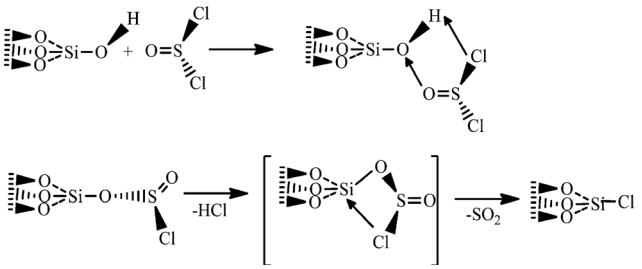

Scheme 1 Synthetic scheme for the preparation of silica chloride.

In view of the comprehensive advantages of silica-supported catalysts, herein we report the stereoselective synthesis of biologically active (*Z*)-acrylonitrile derivatives of substituted chromones and aromatic aldehydes using silica chloride as the heterogeneous catalyst. The efficacy of the catalyst was examined. The catalyst was reused five times and the results show that the catalyst can be reused without a significant reduction of the yield. The compounds were also screened for AChE inhibitory activity against the standard drug tacrine.

2. Results and discussion

2.1. Chemistry

The synthetic pathways of a series of new acrylonitrile derivatives (**2a–i**) and (**4a–c**) are shown in Scheme 2 and 3 respectively. Herein each library (A & B) was typically accessed *via* a facile

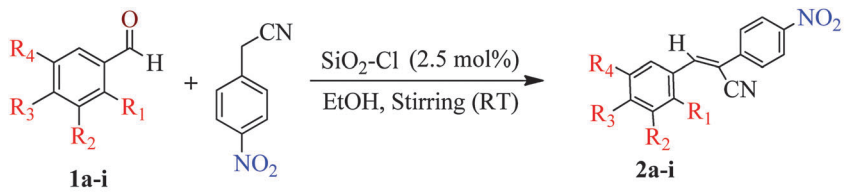

2a (R_1=H; R_2=R_3=R_4=OCH_3)
2b (R_1=R_2=OCH_3; R_3=R_4=H)
2c (R_1=R_3 H; R_2=R_4=OCH_3)
2d (R_1=R_4=H; R_2=R_3=OCH_3)
2e (R_1=R_3=R_4= H; R_2=NO_2)
2f (R_1=R_2=R_4=H; R_3= $N(CH_3)_2$)
2g (R_1=R_4=H; R_2=OCH_3; R_3=OH)
2h (R_1=H; R_2=R_3=R_4=OH)
2i (R_1=R_3=H; R_3=R_4=OH)

Scheme 2 Synthesis of compounds **2a–i**.

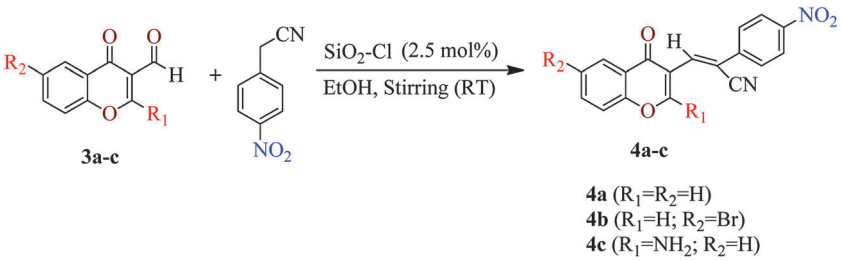

Scheme 3 Synthesis of compounds **4a–c**.

Knoevenagel condensation between *p*-nitrophenylacetonitrile and appropriately substituted aromatic aldehydes (**1a–i**) and 3-formyl chromones (**3a–c**). All of the compounds were obtained in excellent yields (83–92%) with high purity. Among the two possible geometrical isomers (*E*/*Z*), (*Z*)-isomers were obtained as the sole product (Scheme 4). This *Z*-selectivity can be interpreted as a way to minimize steric interactions between the approaching nucleophile (imide form of *p*-nitrophenylacetonitrile) and the bulky substituted aryl substituent and bound catalyst at the crowded, electron deficient carbonyl carbon, favouring back side attack of the nucleophile in such a way that the phenyl ring of the approaching nucleophile is pushed away, thus favouring the formation of the *Z*-isomer. Steric interactions seem to have an influence on the control of the *Z*-configurational isomers. This is further supported by single crystal X-ray crystallographic analysis of compound **2b** and also verified by DFT calculations.

The structural elucidation of the synthesized compounds (**2a–i**) and (**4a–c**) was established on the basis of elemental analysis, IR, ^{1}H NMR, ^{13}C NMR and mass spectral studies. The analytical results for C, H and N were within ±0.3% of the theoretical values. All of the synthesized compounds displayed no peak for the aldehydic carbonyl in the IR spectrum, which confirmed the reaction at the carbonyl moiety. Moreover, all of the compounds displayed a characteristic peak for the cyano group resonating at around 2210–2226 cm^{-1}; similarly, peaks for the nitro group, aromatics (C=C) and other functional moieties are discussed in the experimental section. In the ^{1}H NMR spectra, each compound displayed a sharp singlet at around δ 6.98–8.85 ascribed to the olefinic proton (H-3), and a sharp double doublet appearing at a slightly downfield value δ 8.02–8.34, due to an adjacent electron withdrawing nitro group, corresponds to the H-3″ and H-5″ protons. Similarly, a double doublet at around δ 7.35–7.99 representing two protons

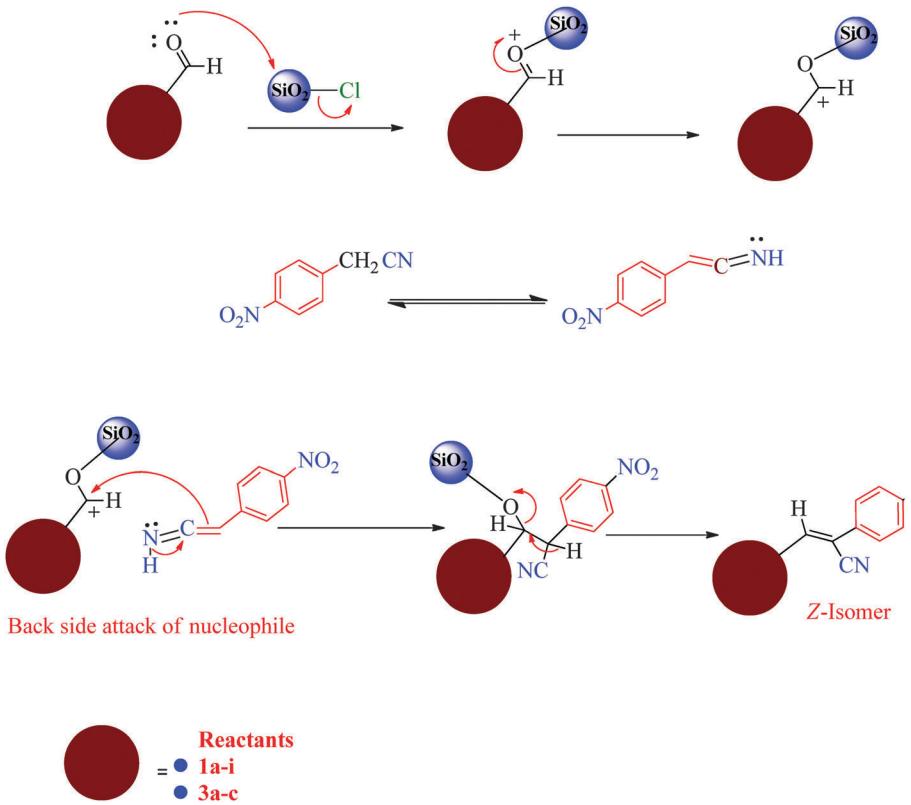

Scheme 4 Plausible mechanism for the synthesis of compounds **2a–i** and **4a–c**.

is attributed to the H-2″ and H-6″ protons and two independent sharp singlets representing one proton each at δ 7.20 and 7.23 are attributed to the H-2′ protons (γ-pyrone ring) of compounds **4b** and **4a** respectively. In the ^{13}C NMR spectra, a series of signals emerging at around δ 109.7–162.3 are ascribed to aromatic carbons, peaks resonating at around δ 115.9–118.4 correspond to the cyanide group and the peaks at δ 177.4, 178.9 and 180.1 correspond the to γ-pyrone ring carbonyl group in the case of compounds **4b**, **4a** and **4c** respectively. The mass spectral analysis was also in agreement with the proposed structure of the compounds.

During the present study, a series of acrylonitrile derivatives of substituted aldehydes (**2a–i**) and substituted 3-formyl chromones (**4a–c**) were synthesized by the Knoevenagel condensation of differently substituted aromatic aldehydes and 3-formyl chromones with *p*-nitrophenylacetonitrile under stirring using piperidine (0.5 mL) as a basic catalyst in ethanol. The reaction took a longer time (4–5 hours) for completion with a moderate yield (67–76%) of the products (Table 1).

In order to develop an eco-friendly approach, we explored the efficacy of silica chloride (SiO_2–Cl) by carrying out the reaction of *p*-nitrophenylacetonitrile with a variety of substituted aromatic aldehydes and 3-formyl chromones in equimolar ratios (1 : 1), in the absence of piperidine at room temperature. The reaction proceeded smoothly and resulted in the formation of the corresponding products (**2a–i**) and (**4a–c**) in good yields (83–92%) within 1.5–2 hours, as monitored by TLC (Table 1). Although the intermediates were not separated and characterized, an attempt was made to establish the mechanism for the formation of (*Z*)-acrylonitrile derivatives **2a–i** and **4a–c** in conformity with the previously reported analogous results (Scheme 4).[58,59] In order to optimize the reaction conditions, a model reaction was conducted using *p*-nitrophenylacetonitrile and 2,3-dimethoxy benzaldehyde (**1b**) under various reaction conditions (including varying the catalyst loading and the effect of the solvent in terms of yields and time). In order to establish the best reaction conditions, we performed an optimization study using a model substrate in the presence of varying amounts of silica chloride. It is clear from Table 2 (entry 5) that 2.5 mol% of the catalyst is sufficient to gain the optimum yield in the shortest reaction time. When using less than 2.5 mol% catalyst (0.5 mol%, 1 mol%, 1.5 mol%, 2 mol%), moderate yields of the product (78–88%) were obtained with higher reaction times, while with an excess mol% of catalyst ($>$2.5 mol%) there was no increase in the yield of the product, probably due to the saturation of the catalyst. In order to study the solvent effect, the model reaction was carried out in different solvent systems. The reaction was primarily tested under solvent-free conditions by the grinding method, however only traces of product were obtained (Table 3, entry 1). When the reaction was performed in CH_2Cl_2 and DMF, moderate yields of the products were obtained after a prolonged reaction period (Table 3, entries 4 and 6), whereas in acetic acid, the reaction again took longer (Table 3, entry 5) but there was an improvement in the yield, probably due to the electromeric effect activating the carbonyl group of the reactants, thus decreasing the activation energy. However, there was a significant improvement in the yield when methanol was used as a solvent (Table 3, entry 3). When the reaction was carried out in EtOH (Table 3, entry 2), the yield of the product improved significantly in a shorter time. A comparative study of a variety of catalysts was conducted to show the superiority of silica chloride as a heterogeneous acid catalyst. When the model reaction was investigated with heterogeneous catalysts such as $HClO_4$–SiO_2, $NaHSO_4$–SiO_2 and NH_4OAc–SiO_2,the reaction required a prolonged time period, and the yields were not satisfactory (Table 4, entries 2–4), whereas using basic catalysts such as piperidine and NaOMe (Table 4, entries 5 and 6), the reaction again took an extended time period for completion, with lower yields, and impure products were obtained. When silica chloride was used as a catalyst (Table 4, entry 1), the yield of the products increased significantly, suggesting silica chloride is the catalyst of choice for the Knoevenagel condensation. The reusability of the silica chloride catalyst was also examined in a model reaction. The catalyst was reused five times and the results show that the catalyst can be reused without a significant reduction of the yield (Table 5). The reusability of the catalyst reduces the cost of the reaction. After the first fresh run with 91% yield, the catalyst was removed by filtration. The recovered catalyst was dried under vacuum at 120 °C for 10 h and tested for five more reaction cycles. Recycling and reuse of the catalyst showed minimal decreases in the yields. The product **2b** was obtained in 90%, 88%, 87%, 85% and 85% yields after successive cycles (Table 5, entries 2–6), thus proving the catalyst's reusability.

2.2. AChE inhibition results

In library A, we analyzed nine aromatic aldehydes, substituted with different groups for AChE inhibition activity. Of the library A analogues (**2a–i**) shown in Table 6, compound **2a**, with a 3,4,5-trimethoxy-substituted benzene moiety (ring A), exhibited the strongest inhibition to AChE with an IC_{50} value of 0.20 μM, followed by compound **2d** (IC_{50} = 0.23 μM), **2f** (IC_{50} = 0.25 μM), **2c** (IC_{50} = 0.27 μM), **2b** (IC_{50} = 0.29 μM), **2h** (IC_{50} = 0.30 μM), **2g** (IC_{50} = 0.35 μM), **2i** (IC_{50} = 0.38 μM) and **2e** (IC_{50} = 0.43 μM). The results indicate that all the tested compounds showed significant AChE inhibitory activity. Among the methoxy-substituted analogues **2a–d**, compound **2a** showed promising activity against AChE inhibition. Compound **2d**, with a 3,4-dimethoxy-substituted benzene ring (ring A), also exhibited encouraging activity but 0.03 lower than **2a**. Similarly, compound **2c**, with methoxy groups at the 3 and 5 positions of the benzene moiety (ring A), showed lower activity than **2d**, while compound **2b**, with methoxy groups at the 2 and 3 positions (ring A), exhibited lower activity than all the 4-methoxy-substituted derivatives. It can be inferred from the data that the position and number of methoxy groups attached to the benzene moiety inflicts a prominent effect on the AChE inhibition. Compound **2a**, with three methoxy groups attached to the benzene moiety (ring A), is the most potent inhibitor. Furthermore, when the methoxy group at the 4 position of the benzene moiety (ring A) in compound **2a** is removed (compound **2c**), the activity decreased significantly by 0.07. Thus the methoxy group at the 4 position in the benzene moiety

Table 1 Silica chloride-catalyzed synthesis of acrylonitrile derivatives **2a–i** and **4a–c**

Derivative	Structure	Reaction in presence of piperidine		Reaction in presence of silica chloride		M.p. (°C)
		Time (hours)	Yield (%)	Time (hours)	Yield (%)	
2a	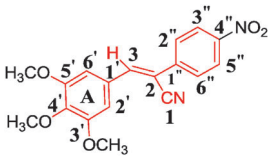	5	69	1.5	87	91–92 (90)[60]
2b	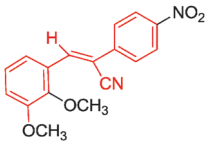	4.5	67	2	91	190–191
2c		5	71	1.7	93	179–180 (180)[60]
2d	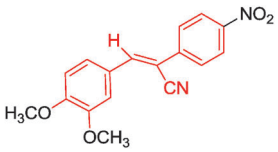	4	73	2	89	152–153
2e	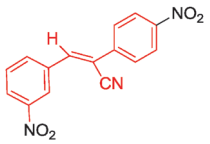	5	67	2	88	178–179
2f	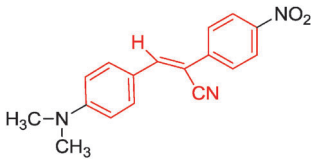	5	70	1.8	85	231–232 (230)[60]
2g	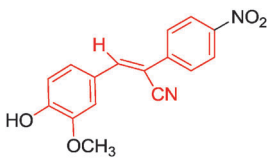	4.6	69	2	87	145–146
2h	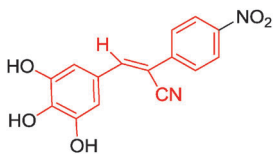	4	68	1.3	84	233–234
2i	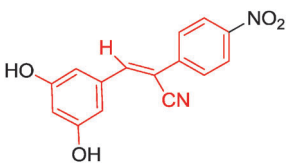	5	67	2	83	181–182
4a	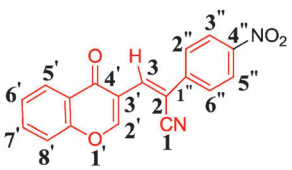	4	76	2	90	194–195

Table 1 (*continued*)

Derivative	Structure	Reaction in presence of piperidine		Reaction in presence of silica chloride		
		Time (hours)	Yield (%)	Time (hours)	Yield (%)	M.p. (°C)
4b	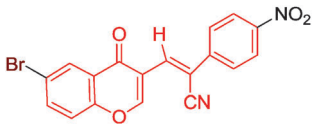	4.3	70	1.5	92	203–204
4c	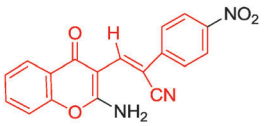	4	69	2	87	187–188

Table 2 Effect of catalyst loading on the synthesis of (**2b**)[a]

Entry	Catalyst (mol%)	Time[b] (hours)	Yield[c] (%)
1	0.5	7	78
2	1.0	6	81
3	1.5	4	85
4	2.0	3	88
5	2.5	2	91
6	3.0	2	91

[a] Reaction conditions: 2,3-dimethoxybenzaldehyde (**1b**,1 mmol), *p*-nitrophenylacetonitrile (1 mmol), stirring, room temperature (25 °C), EtOH solvent. [b] Reaction progress monitored by TLC. [c] Isolated yield of products.

Table 3 Effect of various solvents on a model reaction[a]

Entry	Solvent	Time[b] (hours)	Yield[c] (%)
1	Solvent-free[d]	—	Traces
2	EtOH	2	91
3	MeOH	3.5	83
4	CH_2Cl_2	6	60
5	CH_3COOH	5	69
6	DMF	8	54

[a] Reaction conditions: 2,3-dimethoxybenzaldehyde (**1b**, 1 mmol), *p*-nitrophenylacetonitrile (1 mmol), catalyst (2.5 mol%), different solvents (15 mL), stirring at RT. [b] Reaction progress monitored by TLC. [c] Isolated yield of products. [d] Solvent-free by grinding method.

Table 4 Comparison of the efficiency of silica chloride for the synthesis of (**2b**)[a]

Entry	Catalyst	Time[b] (hours)	Yield[c] (%)
1	Cl–SiO_2	2	91
2	$HClO_4$–SiO_2	5	70
3	$NaHSO_4$–SiO_2	7	68
4	NH_4OAc–SiO_2	6	65
5	Piperidine	4.5	67
6	NaOMe	8	58 (impure)

[a] Reaction conditions: 2,3-dimethoxybenzaldehyde (**1b**, 1 mmol), *p*-nitrophenylacetonitrile (1 mmol), different catalysts (2.5 mol%), EtOH (15 mL), stirring at RT. [b] Reaction progress monitored by TLC. [c] Isolated yield of products.

Table 5 Reusability of the silica chloride catalyst in the synthesis of compound **2b**

Entry	Reaction cycle	Isolated yield (%)
1	1st (fresh run)	91
2	2nd cycle	90
3	3rd cycle	88
4	4th cycle	87
5	5th cycle	85
6	6th cycle	85

Table 6 Quantitative estimation of the acetylcholinesterase inhibition activity of compounds (**2a–i**) by a modified Ellaman's coupled enzyme assay method using tacrine as the reference (n = 3)

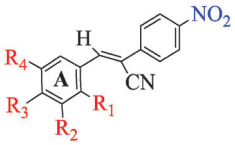

Library A

Entry	Product	Nature of substituents	IC_{50} (μM)[a] ± SEM[b] for *h*AChE[c] inhibition
1	**2a**	R_1 = H; R_2 = R_3 = R_4 = OCH_3	0.20 ± 0.03
2	**2b**	R_1 = R_2 = OCH_3; R_3 = R_4 = H	0.29 ± 0.02
3	**2c**	R_1 = R_3 = H; R_2 = R_4 = OCH_3	0.27 ± 0.05
4	**2d**	R_1 = R_4 = H; R_2 = R_3 = OCH_3	0.23 ± 0.03
5	**2e**	R_1 = R_3 = R_4 = H; R_2 = NO_2	0.43 ± 0.05
6	**2f**	R_1 = R_2 = R_4 = H; R_3 = $N(CH_3)_2$	0.25 ± 0.01
7	**2g**	R_1 = R_4 = H; R_2 = OCH_3; R_3 = OH	0.35 ± 0.03
8	**2h**	R_1 = H; R_2 = R_3 = R_4 = OH	0.30 ± 0.07
9	**2i**	R_1 = R_3 = H; R_3 = R_4 = OH	0.38 ± 0.033
10	Standard (tacrine)	—	0.19 ± 0.02

[a] IC_{50} values represent the concentration of inhibitor required to decrease the enzyme activity by 50%. [b] SEM = standard error of the mean. [c] *h*AChE = human recombinant AChE from human serum was used.

(ring A) is essential for activity. It can also be seen with compounds **2b** and **2d** that although they have two methoxy groups each, compound **2d** with a methoxy group at the 4 position displayed better AChE inhibition in comparison to **2b**. Compound **2f**, with a *N*,*N*-dimethyl $(CH_3)_2N$ substituent attached at the 4 position of the benzene moiety, also showed noteworthy activity, with an IC_{50} value of 0.25 μM. Compound **2e**, with a nitro group at the 3 position (ring A), showed moderate activity among the tested compounds. Compounds **2g–i**, with hydroxy substituents attached to ring A, also showed good

AChE inhibition. Compound **2h**, bearing three hydroxyl groups at the 3, 4 and 5 positions on the benzene moiety (ring A), showed an IC_{50} value of 0.30 μM, with the removal of a hydroxyl group at the 4 position (compound **2i**) significantly lowering its activity by 0.08 in comparison to **2h**. Similarly, compound **2g**, with one of the hydroxyl groups at the 4 position, showed better activity than **2i**, suggesting the vital role of the 4-hydroxyl group for AChE inhibition.

Of the library B analogues (**4a–c**) shown in Table 7, compound **4c** exhibited potent inhibition for AChE with an IC_{50} value of 0.22 μM, followed by compound **4b** (IC_{50} = 0.31 μM) and compound **4a** (IC_{50} = 0.57 μM). The moderate profile of compounds **4a** and **4b** for AChE inhibition is believed to be due to their bulky geometry which restricts them to fit better inside the cavity of AChE.

Table 7 Quantitative estimation of the acetylcholinesterase inhibition activity of compounds (**4a–c**) by a modified Ellaman's coupled enzyme assay method using tacrine as the reference (n = 3)

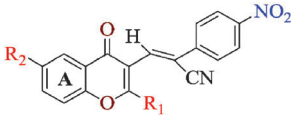

Library B

Entry	Product	Nature of substituents	IC_{50} (μM)[a] ± SEM[b] for *h*AChE[c] inhibition
1	**4a**	$R_1 = R_2 = H$	0.57 ± 0.03
2	**4b**	$R_1 = H$; $R_2 = Br$	0.31 ± 0.05
3	**4c**	$R_1 = NH_2$; $R_2 = H$	0.22 ± 0.04
4	Standard (tacrine)		0.19 ± 0.02

[a] IC_{50} values represent the concentration of inhibitor required to decrease the enzyme activity by 50%. [b] SEM = standard error of the mean. [c] *h*AChE = Human recombinant AChE from human serum was used.

2.3. X-ray crystallographic study

Compound **2b**, once isolated, is found to be air-stable and soluble in all common organic solvents but insoluble in water. X-ray crystallographic analysis reveals that compound **2b** crystallizes in the monoclinic structure with space group $P21/c$. The asymmetric unit of compound **2b** is shown in Fig. 2, while the selected bond lengths and bond angles are listed in Table S1, ESI.† It can be seen that the 3D supramolecular framework of compound **2b** is stabilized *via* an intricate array of H-bonding and weak π···π interactions which are depicted in Fig. 3. Moreover, the packing diagram of compound **2b** is shown in Fig. 4a and b.

2.4. Results of DFT calculations

In order to gain some insight into the influence of the intermolecular interactions on the molecular geometry, we have performed quantum mechanical calculations of the equilibrium geometry of the free molecule. The DFT calculations closely reproduce the solid-state geometry of the molecule. The ground state optimized structure of compound **2b** is shown in Fig. 5a, wherein the dimethoxyphenyl part of the molecule is planar with the acrylic moiety, while the nitrophenyl group is pushed out of the plane, with a dihedral angle of ~27° (C10–C12–C17–C18), probably by the steric interactions between the two hydrogen atoms (H11–H27). The optimized geometry exhibits the (*Z*)-configuration of the dimethoxyphenyl and nitrophenyl groups about the acrylic double bond (Fig. 5a). The HOMO depicts more electronic density over the dimethoxyphenyl rings, with a ground

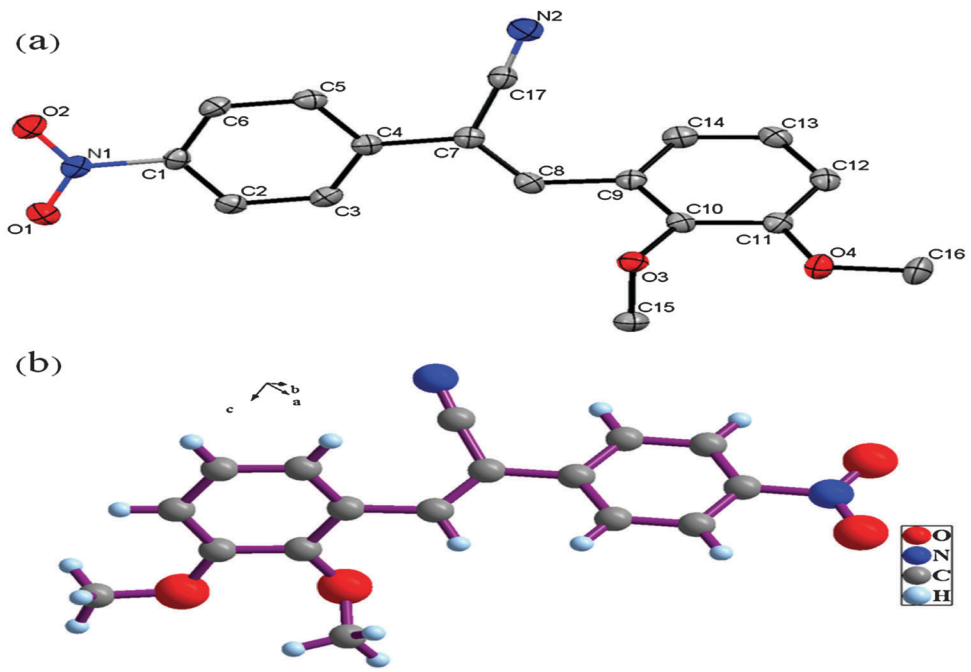

Fig. 2 Asymmetric unit showing (a) thermal ellipsoids (50% probability level). Hydrogen atoms have been omitted for clarity. (b) Ball and stick model of compound **2b**.

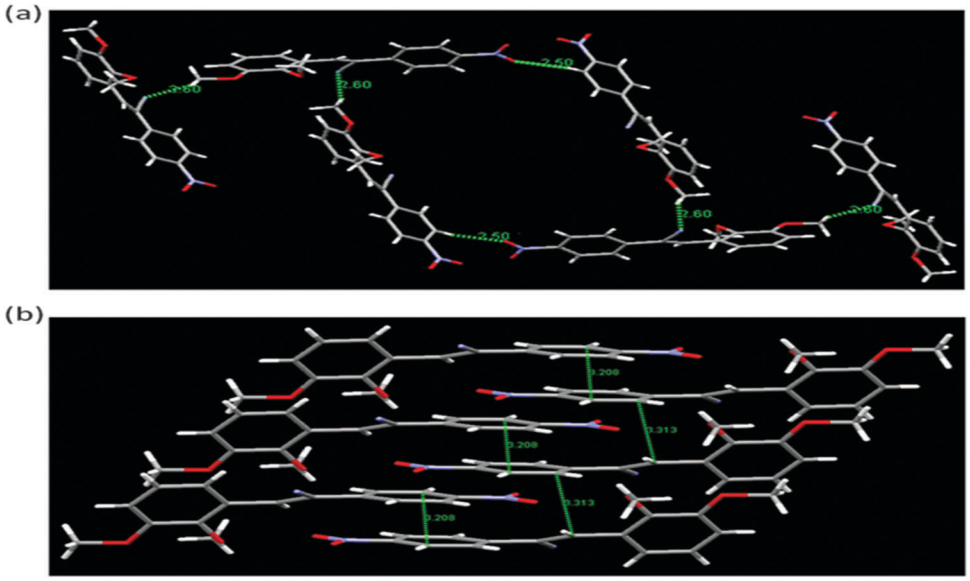

Fig. 3 Representation of (a) H-bonding interactions and (b) π···π interactions in compound **2b**.

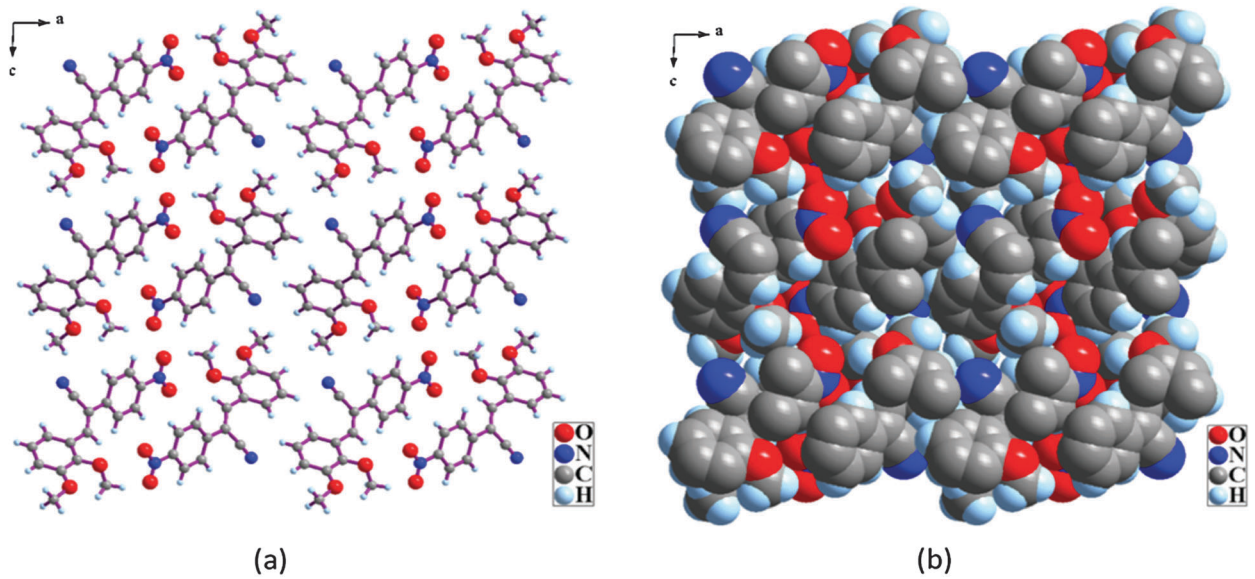

Fig. 4 Packing diagrams of compound **2b**.

state dipole moment vector pointing towards the dimethoxy substituents with a magnitude of 9.49 D suggesting an inhomogeneous distribution of charge in the HOMO (Fig. 6). Single point time-dependent density functional theory calculations of the Franck–Condon state estimated maximum oscillator strength for the HOMO to LUMO transition, with an energy difference of 378 nm. The electronic density is redistributed in the Franck–Condon state as predicted by its distribution in the LUMO, wherein the density is delocalized more towards the nitrophenyl moiety (Fig. 6). Ground state optimization was also carried out for the (*E*)-isomer (Fig. 5b) of this molecule, using the same level of theory, to confirm the relative stability of the two isomers. It was found that the (*Z*)-isomer is stabilized by 2.61 kcal mol^{-1} more than the (*E*)-isomer, and this small energy difference is the reason that during the crystallization process, the (*Z*)-isomer exclusively crystallized out.

Theoretical calculations were also employed to predict the infrared (IR) spectrum of the (*Z*)-form of the molecule (Fig. 7). Based on the vibrational motion corresponding to different spectral lines, various assignments were made. The dominant line at 1363 cm^{-1} corresponds to the stretching frequency of the nitro group. The 1000–1500 cm^{-1} region represents the combined skeletal vibrations of the molecule, and the lines at 1604 cm^{-1} and 1615 cm^{-1} are dominated by the C=C stretching vibration. The CN stretching vibrational mode is observed at 2312 cm^{-1}. These results are nearly in concordance with the experimentally obtained IR spectrum of the molecule (Fig. S1, ESI†).

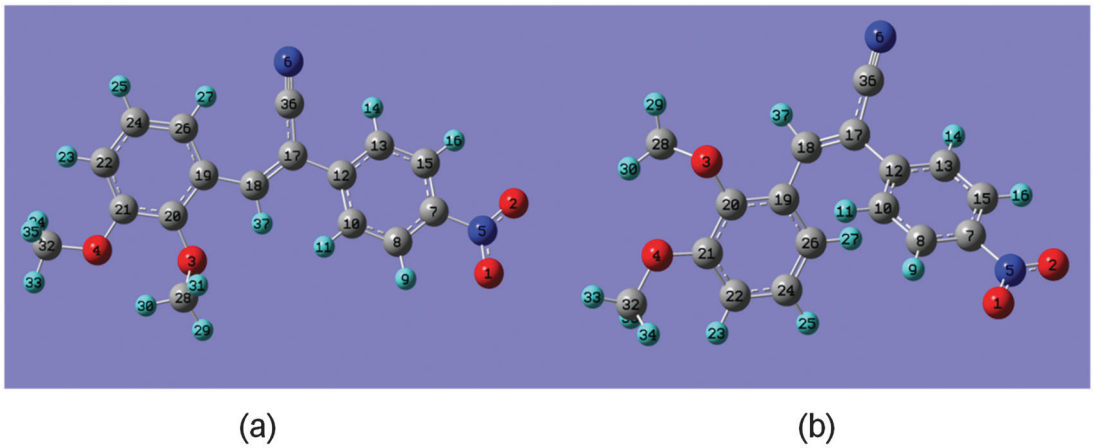

Fig. 5 Ground state optimized structures of the (a) (*Z*)-isomer and (b) (*E*)-isomer of compound **2b**.

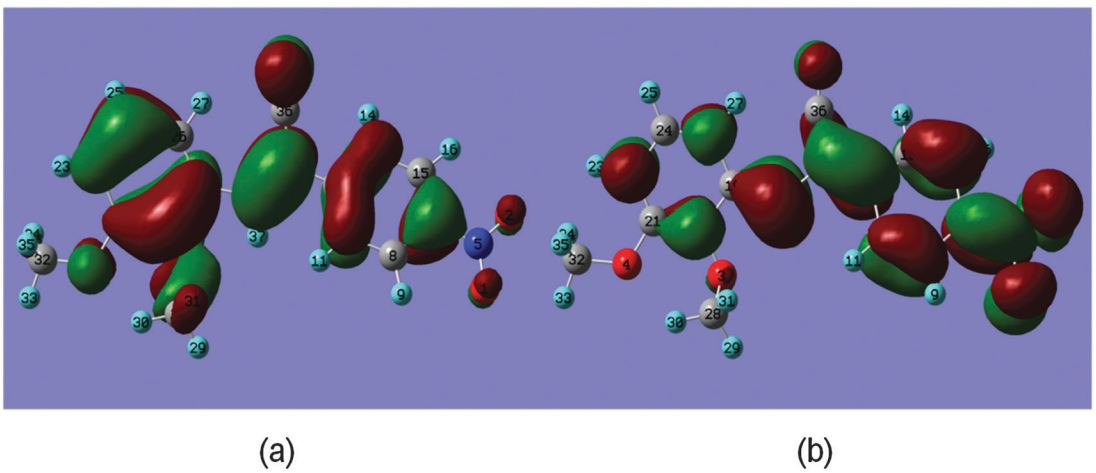

Fig. 6 Electron density distribution in the (a) HOMO and (b) LUMO of the (*Z*)-isomer.

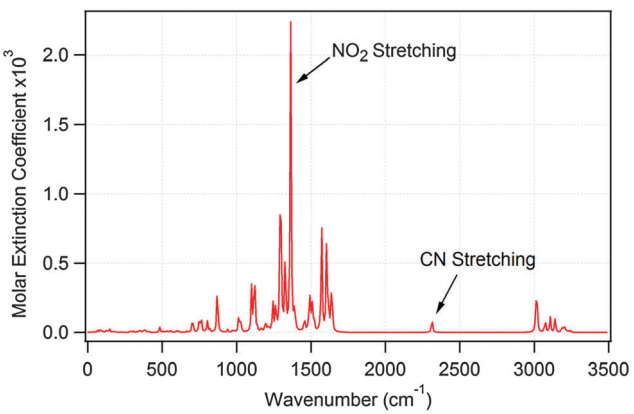

Fig. 7 Theoretically obtained infrared (IR) spectrum of the (*Z*)-isomer by DFT calculations.

3. Conclusions

The present work reports the facile, convenient and eco-friendly, silica chloride-assisted synthesis of (*Z*)-acrylonitrile derivatives (library A & B) of substituted aromatic aldehydes and chromones. The products were obtained in a substantial yield (83–92%) with high purity. The notable features of this procedure are mild reaction conditions, operational simplicity, enhanced reaction rates, cleaner reaction profiles and simple experimental and product separation procedures, which make this method attractive. SAR studies reveal that the position and number of methoxy groups attached to the benzene moiety inflict prominent effects on AChE inhibition. The methoxy group at the 4 position in the benzene moiety (ring A) was found to be obligatory for activity.

4. Experimental section

4.1. Materials and general methods

Chemicals were purchased from Merck and Sigma-Aldrich as 'synthesis grade' and used without further purification. The IR spectra were recorded with a Shimadzu IR-408 Perkin-Elmer 1800 instrument (FTIR), and the values are given in cm^{-1}. ^{1}H NMR and ^{13}C NMR spectra were run in $CDCl_3$ on a Bruker Avance-II 400 MHz instrument with TMS as the internal standard and *J* values measured in Hertz. Chemical shifts are reported in ppm (δ) relative to TMS. Mass spectra were recorded on a JEOL

D-300 mass spectrometer. Melting points were determined on a Kofler apparatus and are uncorrected. Elemental analysis (C, H, N) was conducted using Carlo Erba analyzer model 1108. Thin layer chromatography (TLC) glass plates (20 × 5 cm) were coated with silica gel G (Merck) and exposed to iodine vapor to check the homogeneity as well as the progress of the reaction.

4.2. General method for the synthesis of (*Z*)-2-(4-nitrophenyl)-acrylonitrile derivatives of the substituted aromatic aldehydes

To a mixture of substituted aromatic aldehydes (**1a–i**) and *p*-nitrophenylacetonitrile (1 mmol) in ethanol (20 mL), silica chloride was added (2.5 mol%). The reaction mixture was allowed to stir at room temperature for 1.5–2 hours. During stirring, the clear solution of the reaction mixture began to turn thick, and a solid product precipitated. After completion of the reaction, as evident from TLC, the formed solid was filtered and washed with hot methanol to recover the catalyst. The filtrate containing a soluble product was evaporated under reduced pressure to obtain a crude product. The crude product obtained was washed with appropriate solvents, filtered, dried and crystallized from appropriate solvents. The catalyst was reused without a significant reduction of the yield.

4.2.1. (*Z*)-3-(3′,4′,5′-Trimethoxyphenyl)-2-(4″-nitrophenyl)-acrylonitrile (2a). Compound **2a** recrystallized from $CHCl_3$–MeOH as a brickish red solid. Yield: 87%, m.p. 91–92 °C [lit.,[60] m.p. 90 °C]; anal. calc. for $C_{18}H_{16}N_2O_5$: C, 63.52; H, 4.74; N, 8.23; found: C, 63.54; H, 4.74; N, 8.22. IR ν_{max}^{KBr} cm^{-1}: 2214 (C≡N), 1575, 1456 (C=$C_{aromatic}$), 1508, 1329 (NO_2), 1254 (C–O). ^1H NMR (400 MHz, DMSO, δ, ppm): 8.32 (dd, 2H, H-3″ & H-5″), 7.95 (dd, 2H, H-2″ & H-6″), 7.85 (s, 1$H_{olefinic}$, H-3), 7.21 (s, 2H, H-2′ & H-6′), 3.73 (s, 9H, 3 × OCH_3). ^{13}C NMR (100 MHz, DMSO, δ, ppm): 150.7 (C-3′ & C-5′), 145.4 (C-4″), 143.9 (C-4′), 138.8 (C-1″), 137.3 (C-3), 129.4 (C-2″ & C-6″), 127.4 (C-1′), 124.3 (C-3″ & C-5″), 121.4 (C-2′ & C-6′), 117.6 (C≡N), 106.4 (C-2), 55.7 (OCH_3). MS (ESI) *m*/*z*: 341 $[M+H]^{+\bullet}$.

4.2.2. (*Z*)-3-(2′,3′-Dimethoxyphenyl)-2-(4″-nitrophenyl)-acrylonitrile (2b). Compound **2b** recrystallized from $CHCl_3$–MeOH as bluish crystals. Yield: 91%, m.p. 190–191 °C; anal. calc. for $C_{17}H_{14}N_2O_4$: C, 65.80; H, 4.55; N, 9.03; found: C, 65.80; H, 4.54; N, 9.02. IR ν_{max}^{KBr} cm^{-1}: 2210 (C≡N), 1571, 1476 (C=$C_{aromatic}$), 1511, 1345 (NO_2), 1273 (C–O). ^1H NMR (400 MHz, DMSO, δ, ppm): 8.34 (dd, 2H, H-3″ & H-5″), 8.17 (s, 1$H_{olefinic}$, H-3), 7.97 (dd, 2H, H-2″ & H-6″), 7.18–7.21 (m, 3H, H-4′, H-5′ & H-6′), 3.90 (s, 6H, 2 × OCH_3). ^{13}C NMR (100 MHz, DMSO, δ, ppm): 152.2 (C-3′), 148.3 (C-2′), 147.3 (C-4″), 140.6 (C-1″), 140.1 (C-3), 126.8 (C-2″ & C-6″), 126.7 (C-1′), 123.9 (C-3″ & C-5″), 122.6 (C-5′), 119.2 (C-6′), 116.5 (C≡N), 115.5 (C-4′), 109.9 (C-2), 55.6 (OCH_3). MS (ESI) *m*/*z*: 311 $[M+H]^{+\bullet}$.

4.2.3. (*Z*)-3-(3′,5′-Dimethoxyphenyl)-2-(4″-nitrophenyl)-acrylonitrile (2c). Compound **2c** recrystallized from $CHCl_3$–ethyl acetate as yellowish crystals. Yield: 93%, m.p. 179–180 °C [lit.,[60] m.p. 180 °C]; anal. calc. for $C_{17}H_{14}N_2O_4$: C, 65.80; H, 4.55; N, 9.03; found: C, 65.79; H, 4.54; N, 9.04. IR ν_{max}^{KBr} cm^{-1}: 2215 (C≡N), 1582, 1462 (C=$C_{aromatic}$), 1506, 1338 (NO_2), 1206 (C–O). ^1H NMR (400 MHz, DMSO, δ, ppm): 8.19 (dd, 2H, H-3″ & H-5″), 7.81 (s, 1$H_{olefinic}$, H-3), 7.65 (dd, 2H, H-2″ & H-6″), 7.15 (s, 2H, H-2′ & H-6′), 7.01 (s, 1H, H-4′), 3.71 (s, 6H, 2 × OCH_3). ^{13}C NMR (100 MHz, DMSO, δ, ppm): 162.3 (C-3′ & C-5′), 146.3 (C-4″), 139.5 (C-1″), 138.3 (C-3), 127.3 (C-1′), 125.5 (C-2″ & C-6″), 124.2 (C-3″ & C-5″), 120.6 (C-2′ & C-6′), 117.3 (C≡N), 116.3 (C-4′), 112.6 (C-2), 55.9 (OCH_3). MS (ESI) *m*/*z*: 311 $[M+H]^{+\bullet}$.

4.2.4. (*Z*)-3-(3′,4′-Dimethoxyphenyl)-2-(4″-nitrophenyl)-acrylonitrile (2d). Compound **2d** recrystallized from $CHCl_3$–MeOH as a white creamy solid. Yield: 89%, m.p. 152–153 °C; anal. calc. for $C_{17}H_{14}N_2O_4$: C, 65.80; H, 4.55; N, 9.03; found: C, 65.80; H, 4.56; N, 9.02. IR ν_{max}^{KBr} cm^{-1}: 2224 (C≡N), 1580, 1455 (C=$C_{aromatic}$), 1510, 1335 (NO_2), 1225 (C–O). ^1H NMR (400 MHz, DMSO, δ, ppm): 8.02 (dd, 2H, H-3″ & H-5″), 7.71 (s, 1$H_{olefinic}$, H-3), 7.62 (dd, 2H, H-2″ & H-6″), 6.97 (dd, 2H, H-5′ & H-6′), 6.85 (s, 1H, H-2′), 3.02 (s, 6H, 2 × OCH_3). ^{13}C NMR (100 MHz, DMSO, δ, ppm): 158.6 (C-3′ & C-4′), 147.1 (C-4″), 141.4 (C-1″), 139.7 (C-3), 128.6 (C-1′), 124.9 (C-2″ & C-6″), 124.6 (C-3″ & C-5″), 123.8 (C-2′ & C-5′), 120.1 (C-6′), 118.2 (C≡N), 113.0 (C-2), 57.3 (OCH_3). MS (ESI) *m*/*z*: 311 $[M+H]^{+\bullet}$.

4.2.5. (*Z*)-3-(3′-Nitrophenyl)-2-(4″-nitrophenyl)-acrylonitrile (2e). Compound **2e** recrystallized from $CHCl_3$–acetone as a yellowish solid. Yield: 88%, m.p. 178–179 °C; anal. calc. for $C_{15}H_9N_3O_4$: C, 61.02; H, 3.07; N, 14.23; found: C, 61.03; H, 3.07; N, 14.20. IR ν_{max}^{KBr} cm^{-1}: 2217 (C≡N), 1585, 1445 (C=$C_{aromatic}$), 1520, 1325 (NO_2). ^1H NMR (400 MHz, DMSO, δ, ppm): 8.21 (dd, 2H, H-3″ & H-5″), 8.15 (s, 1H, H-2′), 8.04 (dd, 1H, H-4′), 7.69 (s, 1$H_{olefinic}$, H-3), 7.35 (dd, 2H, H-2″ & H-6″), 7.21 (m, 2H, H-5′ & H-6′). ^{13}C NMR (100 MHz, DMSO, δ, ppm): 148.3 (C-3′ & C-4″), 141.1 (C-1″), 138.4 (C-3), 135.3 (C-1′), 129.5 (C-5′), 127.4 (C-2″ & C-6″), 126.8 (C-3″ & C-5″), 125.7 (C-2′), 125.4 (C-4′), 121.5 (C-6′), 116.9 (C≡N), 109.2 (C-2). MS (ESI) *m*/*z*: 296 $[M+H]^{+\bullet}$.

4.2.6. (*Z*)-3-(4′-Dimethylaminophenyl)-2-(4″-nitrophenyl)-acrylonitrile (2f). Compound **2f** recrystallized from $CHCl_3$–MeOH as a reddish solid. Yield: 85%, m.p. 231–232 °C [lit.,[60] m.p. 230 °C]; anal. calc. for $C_{17}H_{15}N_3O_2$: C, 69.61; H, 5.15; N, 14.33; found: C, 69.60; H, 5.14; N, 14.33. IR ν_{max}^{KBr} cm^{-1}: 2212 (C≡N), 1575, 1447 (C=$C_{aromatic}$), 1513, 1310 (NO_2), 1277 (C–N). ^1H NMR (400 MHz, DMSO, δ, ppm): 8.17 (dd, 2H, H-3″ & H-5″), 7.65 (dd, 2H, H-2″ & H-6″), 7.53 (s, 1$H_{olefinic}$, H-3), 7.25 (dd, 2H, H-2′ & H-6′), 6.58 (dd, 2H, H-3′ & H-5′), 2.78 (s, 6H, 2 × CH_3). ^{13}C NMR (100 MHz, DMSO, δ, ppm): 147.3 (C-4″), 142.5 (C-4′), 141.1 (C-1″), 138.3 (C-3), 127.3 (C-2″ & C-6″), 125.2 (C-3″ & C-5″), 124.8 (C-2′ & C-6′), 121.5 (C-1′), 117.3 (C≡N), 113.4 (C-3′ & C-5′), 108.3 (C-2), 45.3 (CH_3). MS (ESI) *m*/*z*: 294 $[M+H]^{+\bullet}$.

4.2.7. (*Z*)-3-(3′-Methoxy-4′-hydroxyphenyl)-2-(4″-nitrophenyl)-acrylonitrile (2g). Compound **2g** recrystallized from $CHCl_3$–MeOH as a white solid. Yield: 87%, m.p. 145–146 °C; anal. calc. for $C_{16}H_{12}N_2O_4$: C, 64.86; H, 4.08; N, 9.46; found: C, 64.87; H, 4.08; N, 9.44. IR ν_{max}^{KBr} cm^{-1}: 3285 (OH), 2214 (C≡N), 1576, 1440 (C=$C_{aromatic}$), 1504, 1298 (NO_2), 1227 (C–O). ^1H NMR (400 MHz, DMSO, δ, ppm): 9.82 (s, 1H, OH), 8.13 (dd, 2H, H-3″ & H-5″), 7.83 (s, 1$H_{olefinic}$, H-3), 7.67 (dd, 2H, H-2″ & H-6″), 6.81–7.15 (m, 3H, H-2′, H-5′ & H-6′), 3.14 (s, 3H, OCH_3). ^{13}C NMR (100 MHz, DMSO, δ, ppm): 151.4 (C-3′), 145.3 (C-4″), 143.1 (C-4′), 137.6 (C-1″), 135.6 (C-3), 127.6 (C-3″ & C-5″), 125.2 (C-2″ & C-6″), 123.6 (C-1′), 119.4 (C-6′), 118.2 (C≡N), 116.0 (C-5′), 113.2 (C-2′), 106.1 (C-1), 56.8 (OCH_3). MS (ESI) *m*/*z*: 297 $[M+H]^{+\bullet}$.

4.2.8. (*Z*)-3-(3′,4′,5′-Trihydroxyphenyl)-2-(4″-nitrophenyl)-acrylonitrile (2h). Compound **2h** recrystallized from $CHCl_3$–MeOH as a brownish solid. Yield: 84%, m.p. 233–234 °C; anal. calc. for $C_{15}H_{10}N_2O_5$: C, 60.41; H, 3.38; N, 9.39; found: C, 60.40; H, 3.37; N, 9.40. IR ν_{max}^{KBr} cm^{-1}: 3345, 3383 (OH), 2223 (C≡N), 1590, 1445 (C=$C_{aromatic}$), 1494, 1305 (NO_2), 1214 (C–O). ^{1}H NMR (400 MHz, DMSO, δ, ppm): 10.31 (s, OH), 9.34 (s, OH), 8.02 (dd, 2H, H-3″ & H-5″), 7.74 (s, 1$H_{olefinic}$, H-3), 7.61 (dd, 2H, H-2″ & H-6″), 6.97 (s, 2H, H-2′ & H-6′). ^{13}C NMR (100 MHz, DMSO, δ, ppm): 146.6 (C-4″), 145.2 (C-3′ & C-5′), 137.2 (C-1″), 134.1 (C-3), 132.3 (C-4′), 129.7 (C-1′), 127.2 (C-3″ & C-5″), 126.4 (C-2″ & C-6″), 115.9 (C≡N), 112.3 (C-2′ & C-6′), 107.4 (C-2). MS (ESI) *m*/*z*: 299 $[M+H]^{+\bullet}$.

4.2.9. (*Z*)-3-(3′,5′-Dihydroxyphenyl)-2-(4″-nitrophenyl)-acrylonitrile (2i). Compound **2i** recrystallized from $CHCl_3$–ethylacetate as an orange solid. Yield: 83%, m.p. 181–182 °C; anal. calc. for $C_{15}H_{10}N_2O_4$; C, 63.83; H, 3.57; N, 9.92; found: C, 63.84; H, 3.56; N, 9.95. IR ν_{max}^{KBr} cm^{-1}: 3387, 3312 (OH), 2216 (C≡N), 1583, 1460 (C=$C_{aromatic}$), 1485, 1315 (NO_2), 1217 (C–O). ^{1}H NMR (400 MHz, DMSO, δ, ppm): 9.87 (s, OH), 8.14 (dd, 2H, H-3″ & H-5″), 7.75 (s, 1$H_{olefinic}$, H-3), 7.63 (dd, 2H, H-2″ & H-6″), 6.97 (s, 2H, H-2′ & H-6′), 6.75 (s, 1H, H-4′). ^{13}C NMR (100 MHz, DMSO, δ, ppm): 154.7 (C-3′ & C-5′), 144.8 (C-4″), 141.2 (C-1″), 138.5 (C-3), 127.3 (C-3″ & C-5″), 125.9 (C-2″ & C-6″), 124.8 (C-2′ & C-6′), 121.6 (C-1′), 118.4 (C≡N), 109.7 (C-4′), 107.5 (C-2). MS (ESI) *m*/*z*: 283 $[M+H]^{+\bullet}$.

4.3. General method for the synthesis of (*Z*)-2-(4-nitrophenyl)-acrylonitrile derivatives of substituted 3-formyl chromones

To a mixture of substituted 3-formyl chromones (**3a–c**) and *p*-nitrophenylacetonitrile (1 mmol) in ethanol (20 mL), silica chloride was added (2.5 mol%). The reaction mixture was allowed to stir at room temperature for 1.5–2 hours. The clear solution of the reaction mixture began to turn thick and the solid product began to settle out. After completion of the reaction, as evident from TLC, the formed solid was filtered and washed with hot methanol to recover the catalyst. The filtrate containing the soluble product was evaporated under reduced pressure to obtain the crude product. The crude product was washed with appropriate solvents, filtered, dried and crystallized from appropriate solvents. The catalyst was reused without significant reduction of the yield.

4.3.1. (*Z*)-3-(4′-Oxo-4*H*-chromen-3-yl)-2-(4″-nitrophenyl)-acrylonitrile (4a). Compound **4a** recrystallized from $CHCl_3$–MeOH as a yellowish solid. Yield: 90%, m.p. 194–195 °C; anal. calc. for $C_{18}H_{10}N_2O_4$: C, 67.92; H, 3.17; N, 8.80; found: C, 67.93; H, 3.19; N, 8.81. IR ν_{max}^{KBr} cm^{-1}: 2218 (C≡N), 1650 (C=$O_{\gamma\text{-pyrone}}$), 1610 (C=$C_{\gamma\text{-pyrone}}$), 1563, 1464 (C=$C_{aromatic}$), 1515, 1341 (NO_2). ^{1}H NMR (400 MHz, DMSO, δ, ppm): 8.32 (dd, 2H, H-3″ & H-5″), 7.99 (dd, 2H, H-2″& H-6″), 7.85 (dd, 2H, H-5′ & H-8′), 7.65 (s, 1$H_{olefinic}$, H-3), 7.37 (dd, 2H, H-6′ & H-7′), 7.23 (s, 1H, H-2′). ^{13}C NMR (100 MHz, DMSO, δ, ppm): 178.9 (C-4′), 162.5 (C-2′), 155.2 (C-8a), 147.3 (C-4″), 139.2 (C-1″), 136.8 (C-2), 134.3 (C-7′), 129.7 (C-2″ & C-6″), 125.5 (C-6′), 124.8 (C-5′), 123.6 (C-4a), 122.4 (C-3″ & C-5″), 118.6 (C-8′), 117.2 (C≡N), 116.3 (C-3), 110.5 (C-3′). MS (ESI) *m*/*z*: 318 $[M+H]^{+\bullet}$.

4.3.2. (*Z*)-3-(6′-Bromo-4′-oxo-4*H*-chromen-3-yl)-2-(4″-nitrophenyl)-acrylonitrile (4b). Compound **4b** recrystallized from $CHCl_3$–acetone as a grayish white solid. Yield: 92%, m.p. 203–204 °C; anal. calc. for $C_{18}H_9BrN_2O_4$: C, 54.43; H, 2.28; N, 7.05; found: C, 54.43; H, 2.27; N, 7.04. IR ν_{max}^{KBr} cm^{-1}: 2226 (C≡N), 1650 (C=$O_{\gamma\text{-pyrone}}$), 1599 (C=$C_{\gamma\text{-pyrone}}$), 1464 (C=$C_{aromatic}$), 1519, 1341 (NO_2), 599 (C–Br). ^{1}H NMR (400 MHz, DMSO, δ, ppm): 8.01 (dd, 2H, H-3″ & H-5″), 7.91 (dd, 2H, H-2″& H-6″), 7.82 (s, 1H, H-5′), 7.61 (s, 1$H_{olefinic}$, H-3), 7.32 (dd, 2H, H-7′ & H-8′), 7.20 (s, 1H, H-2′). ^{13}C NMR (100 MHz, DMSO, δ, ppm): 177.4 (C-4′), 161.2 (C-2′), 155.8 (C-8a), 145.2 (C-4″), 140.1 (C-1″), 137.8 (C-2), 133.7 (C-7′), 130.8 (C-2″ & C-6″), 128.3 (C-6′), 124.1 (C-5′), 123.9 (C-4a), 120.7 (C-3″ & C-5″), 119.0 (C-8′), 117.8 (C≡N), 112.4 (C-3), 110.1 (C-3′). MS (ESI) *m*/*z*: 397 $[M+H]^{+\bullet}$.

4.3.3. (*Z*)-3-(2′-Amino-4-oxo-4*H*-chromen-3-yl)-2-(4″-nitrophenyl)-acrylonitrile (4c). Compound **4c** recrystallized from $CHCl_3$–MeOH as a brownish solid. Yield: 87%, m.p. 187–188 °C; anal. calc. for $C_{18}H_{11}N_3O_4$: C, 64.86; H, 3.33; N, 12.61; found: C, 64.86; H, 3.32; N, 12.60. IR ν_{max}^{KBr} cm^{-1}: 3492 (NH_2), 2223 (C≡N), 1631 (C=$O_{\gamma\text{-pyrone}}$), 1603 (C=$C_{\gamma\text{-pyrone}}$), 1555, 1464 (C=$C_{aromatic}$), 1515, 1345 (NO_2). ^{1}H NMR (400 MHz, DMSO, δ, ppm): 8.34 (dd, 2H, H-3″ & H-5″), 7.97 (dd, 2H, H-2″ & H-6″), 7.89 (s, 2H, NH_2, D_2O exchangeable), 7.23–7.85 (m, 4H, H-5′, H-6′, H-7′ & H-8′), 6.98 (s, 1$H_{olefinic}$, H-3). ^{13}C NMR (100 MHz, DMSO, δ, ppm): 180.1 (C-4′), 166.8 (C-2′), 154.7 (C-8a), 144.2 (C-4″), 142.3 (C-1″), 138.1 (C-2), 131.5 (C-7′), 130.4 (C-2″ & C-6″), 129.1 (C-6′), 125.6 (C-5′), 123.4 (C-4a), 121.2 (C-3″ & C-5″), 118.3 (C-8′), 116.4 (C≡N), 114.2 (C-3), 112.7 (C-3′). MS (ESI) *m*/*z*: 334 $[M+H]^{+\bullet}$.

4.4. Single crystal X-ray crystallographic studies of compound 2b

Single crystal X-ray data of compound **2b** was collected at 100 K on a Bruker SMART APEX CCD diffractometer using graphite monochromated MoK_α radiation (λ = 0.71073 Å). The linear absorption coefficients, scattering factors for the atoms and the anomalous dispersion corrections were taken from the International Tables for X-ray Crystallography.[61] The data integration and reduction were carried out with SAINT software.[62] An empirical absorption correction was applied to the collected reflections with SADABS, and the space group was determined using XPREP.[63] The structure was solved by direct methods using SHELXTL-97 and refined on F^2 by full-matrix least-squares using the SHELXL-97[64] program package. All non-hydrogen atoms were refined anisotropically. Pertinent crystallographic data for compound **2b** is summarized in Table 8.

4.5. Density functional theory (DFT) calculations

Quantum mechanical calculations were pursued for the molecule **2b**, the crystal structure of which has been discussed. The B3LYP functional and 6-311+g(d,p) basis set were used to carry out the ground state optimization of the molecule in the Gaussian 09 software package.[65] A vibrational analysis was performed for compound **2b** to calculate the IR spectrum. We also calculated the single point energy for the optimized structures of the (*Z*)- and (*E*)-conformations of compound **2b** using the B3LYP/6-311+g(d,p) level of theory.

4.6. *In vitro* acetylcholinesterase inhibition activity

The ability of compounds (**2a–i**) and (**4a–c**) to inhibit AChE activity was assessed by Ellman's method.[66] AChE stock solution

Table 8 Crystallographic data and structure refinement of compound **2b**

Compound	**2b**
Empirical formula	$C_{17}H_{14}N_2O_4$
Formula wt	310.30
Crystal system	Monoclinic
Space group	$P21/c$
a (Å)	15.634(5)
b (Å)	4.720(2)
c (Å)	19.585(5)
α (°)	90
β (°)	91.229(5)
γ (°)	90
U (Å^3)	1444.9(16)
Z	4
ρ_{calc} (Mg m^{-3})	1.426
μ (mm^{-1})	0.103
F(000)	648
Refl. collected	7121
Independent refl.	2178
GOF	1.129
Final R indices	$R_1 = 0.0494^a$
$[I > 2\sigma(I)]$	$wR_2 = 0.1345^b$
R indices	$R_1 = 0.0633$
(all data)	$wR_2 = 0.1712$

^{a} $R_1 = \sum||F_o| - |F_c||/\sum|F_o|$ with $F_o^2 > 2\sigma(F_o^2)$. ^{b} $wR_2 = [\sum w(|F_o^2| - |F_c^2|)^2/\sum|F_o^2|^2]^{1/2}$.

was prepared by dissolving human recombinant AChE (E.C.3.1.1.7) lyophilized powder (Sigma Aldrich) in 0.1 M phosphate buffer (pH = 8.0) containing Triton X-100 (0.1%). Five increasing concentrations of test compounds were assayed to obtain the % inhibition of the enzymatic activity in the range of 20–80. The assay solution consisted of a 0.1 M phosphate buffer (pH 8.0), with the addition of 340 μM 5,5′-dithio-bis(2-nitrobenzoic acid), 0.02 units per mL of human recombinant AChE from human serum and 550 μM of substrate (acetylthiocholine iodide, ATCh). Increasing concentrations of the tested inhibitor were added to the assay solution and pre-incubated for 20 min at 37 °C with the enzyme, followed by the addition of the substrate. Initial rate assays were performed at 37 °C with a Jasco V-530 double beam spectrophotometer. The absorbance value at 412 nm was recorded for 5 min and the enzyme activity was calculated from the slope of the obtained linear trend. Assays were carried out with a blank containing all of the components except AChE to account for the non-enzymatic reaction. The reaction rates were compared and the percent inhibition due to the presence of the tested inhibitors was calculated. Each concentration was analyzed in triplicate, and the IC_{50} values were determined graphically from log concentration–inhibition curves (GraphPad Prism 4.03 software, GraphPad Software Inc.). Tacrine was used as a standard inhibitor. The AChE inhibition activity of the synthesized compounds is presented in Tables 6 and 7.

Acknowledgements

A. Mohammed thanks the Chairman, Department of Chemistry, A.M.U., Aligarh, for providing the necessary research facilities, and the UGC is also gratefully acknowledged for the research fellowship. The CSIR, New Delhi, is also thanked for the award of the Research Associateship to M. Alam.

References

1 E. Knoevenagel, *Ber. Dtsch. Chem. Ges.*, 1898, **31**, 2585–2596.
2 F. Bigi, L. Chesini, R. R. Maggi and G. Sartori, *J. Org. Chem.*, 1999, **64**, 1033–1035.
3 N. Yu, J. M. Aramini, M. W. Germann and Z. Huang, *Tetrahedron Lett.*, 2000, **41**, 6993–6996.
4 G. Jones, The Knoevenagel condensation reaction, *Organic Reactions*, Wiley, New York, 1967, vol. 15, p. 204.
5 L. F. Tietze and U. Beifuss, *Comprehensive Organic Synthesis*, Pergamon, New York, 1991, vol. 2, pp. 341–394.
6 S. M. J. Mukarram, R. A. R. Khan and R. P. Yadav, *US Pat.*, 0004935, 2007.
7 L. R. Madivada, R. R Anumala, G. Gilla, S. Alla, K. Charagondla, M. Kagga, A. Bhattacharya and R. Bandichhor, *Org. Process Res. Dev.*, 2009, **13**, 1190–1194.
8 U. Beutler, P. C. Fuenfschilling and A. Steinkemper, *Org. Process Res. Dev.*, 2007, **11**, 470–476.
9 A. Carta, P. Sanna, M. Palomba, L. Vargiub, M. La Colla and R. Loddo, *Eur. J. Med. Chem.*, 2002, **37**, 891–900.
10 A. Carta, I. Briguglio, S. Piras, G. Boatto, P. L. Colla, R. Loddo, M. Tolomeo, S. Grimaudo, A. D. Cristina, R. M. Pipitone, E. Laurini, M. S. Paneni, P. Posocco, M. Fermeglia and S. Pricl, *Eur. J. Med. Chem.*, 2011, **46**, 4151–4167.
11 K. M. Dawood, N. M. Elwan, A. A. Farahat and B. F. Abdel-Wahab, *J. Heterocycl. Chem.*, 2010, **47**, 243–267.
12 A. Carta, M. Palomba, G. Boatto, B. Busonera, M. Murreddu and R. Loddo II, *Farmaco*, 2004, **59**, 637–644.
13 J. Quiroga, D. Cobo, B. Insuasty, R. Abonía, M. Nogueras, J. Cobo, Y. Vasquez, M. Gupta, M. Derita and S. Zacchino, *Arch. Pharm.*, 2007, **340**, 603–606.
14 M. Hranjec, G. Pavlovic, M. Marjanovic, M. Kralj and G. Karminski-Zamola, *Eur. J. Med. Chem.*, 2010, **45**, 2405–2417.
15 F. Saczewski, A. Stencel, A. M. Bienczak, K. A. Langowska, M. Michaelis, W. Werel, R. Halasa, P. Reszka and P. Bednarski, *Eur. J. Med. Chem.*, 2008, **43**, 1847–1857.
16 P. Sanna, A. Carta and M. E. R. Nikookar, *Eur. J. Med. Chem.*, 2000, **35**, 535–543.
17 V. S. Parmar, A. Kumar, A. K. Prasad, S. K. Singh, N. Kumar, S. Mukherjee, H. G. Raj, S. Goel, W. Errington and M. S. Puard, *Bioorg. Med. Chem.*, 1999, **7**, 1425–1436.
18 S. A. Shiba, *Phosphorus, Sulfur Silicon Relat. Elem.*, 1996, **114**, 29–37.
19 S. Naruto, H. Mizuta, T. Yoshida, H. Uno, K. Kawashima, T. Kadokawa and H. Nishimura, *Chem. Pharm. Bull.*, 1983, **31**, 3022–3032.
20 J. Grundy, *Chem. Rev.*, 1957, **57**, 281–415.
21 W. Kuzmierkiewicz, H. Foks and M. Baranowski, *Sci. Pharm.*, 1985, **53**, 133–138.
22 P. Sanna, A. Carta, L. Gherardini and M. E. R. Nikookar II, *Farmaco*, 2002, **57**, 79–87.
23 E. A. Glazer and L. R. Chappel, *J. Med. Chem.*, 1982, **25**, 766–769.
24 L. Quattara, M. Debaert and R. Cavier, *Farmaco, Ed. Sci.*, 1987, **42**, 383–396.
25 A. Repicky, S. Jantova and L. Cipak, *Cancer Lett.*, 2009, **277**, 55–63.

26 P. D. L Torre, L. A. Saavedra, J. Caballero, J. Quiroga, J. H. Alzate-Morales, M. G. Cabrera and J. Trilleras, *Molecules*, 2012, **17**, 12072–12085.
27 L. W. Yi, X. Q. Hai, M. Y. Xiang, L. Y. Min, D. N. Li and G. D. Peng, *J. Org. Chem.*, 2001, **625**, 128–131.
28 S. El-Tammany, F. W. Raulfs and H. Hopf, *Angew. Chem., Int. Ed. Engl.*, 1983, **22**, 633–634.
29 J. Masllorens, M. M. Manas, A. P. Quintana, R. Pleixats and A. Roglans, *Synthesis*, 2002, **13**, 1903–1911.
30 D. S. Acker and W. R. Hertler, *J. Am. Chem. Soc.*, 1962, **84**, 3370–3374.
31 S. Sebti, A. Smahi and A. Solhy, *Tetrahedron Lett.*, 2002, **43**, 1813–1815.
32 P. Verdía, F. Santamarta and E. Tojo, *Molecules*, 2011, **16**, 4379–4388.
33 A. Akbari, M. Amirabedi and B. E. Sis, *J. Chem. Chem. Eng.*, 2012, **6**, 658–660.
34 F. Bigi, L. Chesini, R. Maggi and G. Sartori, *J. Org. Chem.*, 1999, **64**, 1033–1035.
35 R. V. Hangarge, S. A. Sonwane, D. V. Jarikote and M. S. Shingare, *Green Chem.*, 2001, **3**, 310–312.
36 M. L. Deb and P. J. Bhuyan, *Tetrahedron Lett.*, 2005, **46**, 6453–6456.
37 G. Thirupathi, M. Venkatanarayana, P. K. Dubey and Y. B. Kumari, *Der Pharma Chem.*, 2012, **4**, 1897–1901.
38 M. Tarleton, J. Gilbert, J. A. Sakoff and A. McCluskey, *Eur. J. Med. Chem.*, 2012, **57**, 65–73.
39 J. S. Biradar and B. S. Sasidhar, *Eur. J. Med. Chem.*, 2011, **46**, 6112–6118.
40 B. Karmakar, A. Nayak and J. Banerji, *Tetrahedron Lett.*, 2012, **53**, 4343–4346.
41 M. S. Abaee, M. M. Mojtahedi, M. M. Zahedi and G. Khanalizadeh, *ARKIVOC*, 2006, **xv**, 48–52.
42 J. S. Yadav, P. P. Rao, D. Sreenu, R. S. Rao, V. N. Kumar, K. Nagaiah and A. R. Prasad, *Tetrahedron Lett.*, 2005, **4**, 7249–7253.
43 F. Nemati, M. M. Heravi and R. S. Rad, *Chin. J. Catal.*, 2012, **33**, 1825–1831.
44 C. Mukhopadhyay and S. Ray, *Catal. Commun.*, 2011, **12**, 1496–1502.
45 F. Xu, D. Q. Yang, K. L. Jiyang and W. Guo, *Chin. Chem. Lett.*, 2006, **17**, 187–190.
46 V. Aldabalde, M. Risso, M. L. Derrudi, F. Geymonat, G. Seoane, D. Gamenara and P. Saenz-Mendez, *Open J. Phys. Chem.*, 2011, **1**, 85–93.
47 Q. Liu, H. Ai and Z. Li, *Ultrason. Sonochem.*, 2011, **18**, 477–479.
48 H. Guo, X. Liu, Q. Xie, L. Wang, D. L. Peng, P. S. Branco and M. B. Gawande, *RSC Adv.*, 2013, **3**, 19812–19815.
49 S. Minakata and M. Komatsu, *Chem. Rev.*, 2009, **109**, 711–724.
50 M. B. Gawande, V. Polshettiwar, R. S. Varma and R. V. Jayarama, *Tetrahedron Lett.*, 2007, **48**, 8170–8173.
51 H. Firouzabadi, N. Iranpoor, H. Hazarkhani and B. Karimi, *J. Org. Chem.*, 2002, **67**, 2572–2576.
52 L. Q. Wu, L. M. Yang, X. Wang and F. L. Yan, *J. Chin. Chem. Soc.*, 2010, **57**, 738–741.
53 R. Karimian, F. Piri, A. A. Safari and S. J. Davarpanah, *J. Nanostruct. Chem.*, 2013, **3**, 52.
54 Y. Kamitori, M. Hojo, R. Masuda, T. Kimura and T. Yoshida, *J. Org. Chem.*, 1986, **51**, 1427–1431.
55 Y. I. Gorlov, A. M. Nesterenko and A. A. Chuiko, *Colloids Surf., A*, 1996, **106**, 83–88.
56 M. B. Gawande, P. S. Brancoa and R. S. Varma, *Chem. Soc. Rev.*, 2013, **42**, 3371–3393.
57 M. B. Gawande, A. K. Rathi, I. D. Nogueira, R. S. Varma and P. S. Branco, *Green Chem.*, 2013, **15**, 1895–1899.
58 F. W. Upson, R. T. Maxwell and H. M. Parmelee, *J. Am. Chem. Soc.*, 1930, **52**, 1971–1975.
59 H. N. Karade, M. Sathe and M. P. Kaushik, *Molecules*, 2007, **12**, 1341–1351.
60 A. M. Asiri, *Pigm. Resin Technol.*, 2004, **33**, 370–374.
61 *International Tables for X-Ray Crystallography*, Kynoch Press, Birmingham, England, 1952, vol. III.
62 *SAINT, Version 6.02*, Bruker AXS, Madison, WI, 1999.
63 *XPREP, Version 5.1*, Siemens Industrial Automation Inc., Madison, WI, 1995.
64 G. M. Sheldrick, *SHELXL-97: Program for Crystal Structure Refinement*, University of Göttingen, Göttingen, Germany, 1997.
65 M. J. Frisch, *et al.*, *Gaussian 09, Revision A.1*, Gaussian, Inc., Wallingford CT, 2009.
66 G. L. Ellman, K. D. Courtney, V. J. Andres and R. M. Feather-Stone, *Biochem. Pharmacol.*, 1961, **7**, 88–90.